Magnetic Storms and Associated Interplanetary Phenomena

Bruce T. Tsurutani
Space Physics and Astrophysics Section
Jet Propulsion Laboratory, California Institute of Technology
Pasadena, California, 91109

Walter D. Gonzalez
Instituto Nacional Pesquisas Espaciais
Sao Jose (los Campos
San Paulo, Brazil

0/()"//)0

Abstract

The physical mechanism for energy transfer from the solar wind to the magnetosphere is magnetic reconnection between the interplanetary field and the earth's field. During and a few years after solar maximum, the dominant interplanetary phenomena causing intense magnetic storms ($D_{ST} < -100$ nT) are the interplanetary manifestations of fast coronal mass ejections (CMEs). Two interplanetary regions are important for intense southward IMFs: the sheath region just behind the forward shock, and the ejecta material itself. Whereas the initial phase of a storm is caused by the increase in plasma ram pressure associated with the increase in density and speed at and behind the shock (accompanied by a sudden impulse [SI] at Earth), the storm main phase is due to southward IMFs. If the fields are southward in both of the sheath and solar ejecta, two-step main phase storms can result. The storm recovery phase begins when the IMF turns less southward, with delays of ~1-2 hours. The recovery phase has a decay time of ~10 hours and is physically due to a combination of several different energetic particle loss processes (Coulomb collisions, charge exchange and wave-particle interactions). During solar minimum, high speed streams from coronal holes dominate the interplanetary medium activity. The high-density, low-speed streams associated with the heliospheric current sheet (HCS) plasmasheet impinging upon the Earth's magnetosphere cause positive D_{ST} values (storm initial phases if followed by main phases). In the absence of shocks, SIs are infrequent during this phase of the solar cycle. High-field regions called Corotating Interaction Regions (CIRs) are created by the fast stream (emanating from the coronal hole) interaction with the HCS plasmasheet. However, because the B_z component is typically highly fluctuating within the CIRs, the main phases of the resultant magnetic storms typically have highly irregular profiles and are weaker. Storm recovery phases during this phase of the solar cycle are also quite different in that they can last from many days to weeks. The southward magnetic field (B_s) component of Alfvén waves in the high speed stream proper cause intermittent reconnection, intermittent substorm activity, and sporadic injections of plasmasheet energy into the outer portion of the ring current, prolonging its final decay to quiet day values. This continuous auroral activity is called high intensity long duration continuous AE activity (HILDCAAs).

INTRODUCTION

The primary cause of magnetic storms are intense, long-dura tion southward interplanet ary magnetic fields which interconnect with the earth's magnetic field and allow solar wind energy transport into the earth's magnetotail/magnetosphere. It is the purpose of this paper to review the

sources of such interplanetary magnetic fields distinguishing between the solar maximum and the declining phases of the solar cycle.

The solar wind speed, V_{sw}, plays an equal role in the interplanetary cross tail electric field ($-V_{sw} \times B_s/c$). However, it is found empirically that the solar wind speed is usually only a minor factor for the creation of storms. The reason for this is that the variability of the magnitude of the solar wind speed is much less than the variability of the magnitude of B_s.

Solar Maximum

During the most active phase of the solar cycle, solar maximum, the sun's activity is dominated by flares and disappearing filaments, and their concomitant Coronal Mass Ejections (CMEs). Coronal holes are present, but the holes are small and do not extend fl'oil) the poles to the equator as often happens in the descending phase of the solar cycle. However, Gonzalez et al. (1996) and Bravo et al. (1996) have indicated possible roles for these small coronal holes. WC refer the reader to these articles for further details.

The fast (>500 km s^{-1}) CMEs coming from the sun into interplanetary space are the solar/coronal features that contain high magnetic fields. Figure 1 is a schematic of the remnants of such a solar ejecta detected at 1 AU. (Each of the three main identifying features of CMEs observed close to the sun have not been identified at 1 AU, see Tsurutani and Gonzalez, 1995a for details). There are two principal regions of intense fields. If the speed differential between the coronal ejecta and the slow, upstream solar wind is greater than the magnetosonic wave speed (50-70 km s^{-1}), a forward shock is formed. The larger the differential speed, the stronger the Mach number of the shock. The average interplanetary quiet field is 3-8 nT and shock compression (magnetic field jump) across the shock of this field is roughly proportional to the Mach number. Interplanetary shocks typically have Mach numbers of 2-3, so the interplanetary "sheath" fields downstream of the shock are typically up to 9-24 nT. In exceptional events, the speed differential is larger than Mach 4, and a maximum compression in the field of ~4 is attained.

The primary part of the solar ejects might contains a so-called magnetic cloud (Burlaga et al. 19S 1: 1987; Klein and Burlaga, 1982; Lepping et al. 1 990; Farrugia et al., 1993 a, b). The magnetic cloud is a region of slowly varying and strong magnetic fields (10-25 nT or higher) with exceptionally low plasma beta, typically ~0. 1 (Choe et al., 1992; Tsurutani and Gonzalez, 1995:1: this is particular nicely shown in Farrugia et al.,1993a,Figure 4). The magnetic field often has a north-to-south (or vice versa) rotation to it (Figure 2 and is elongated along its axis, forming a

giant flux rope [Farrugia, this issue]). Whether these fields remain connected to the sun or not is currently being debated.

Other three-dimensional shapes, such as spherical, toroidal Or cylindrical forms, have been explored as well (Ivanov et al., 1 989; Vandas et al., 1991, 1993; Farrugia et al., 1995). Simple configurations such as the so called "magnetic tongues" proposed by Gold (1 962) have been sought in this study, but were not found in the ISEE-3 1978-79 data set.

At the present time we have not identified all of the component pieces of a CME at 1 AU as indicated in Figure 1. A "classic" CME is shown in Figure 3, courtesy of A. Hundhausen. This is a Solar Maximum Mission white-light coronagraph image. The time sequence goes from left to right. The three parts of a CME are illustrated in the left panel. Furthest from the sun are bright outer loops. Next is a dark region, and closest to the sun are bright twisted filaments. It has been speculated by Tsurutani and Gonzalez (1995a) that the magnetic cloud most probably corresponds to the central, dark region of the CME. This is because magnetic clouds are characterized by low temperature plasma. If the above argument is correct, then where are the loops and filaments? A hint can be found in Figure 4, taken from Galvin et al. (1987). A magnetic cloud is present in the ISEE-3 data from 0830 to 1800 UT. It is characterized by high fields (peak of ~25 nT), a rotation from a southward direction to a northward direction (bottom panel), and a lack of Alfvén waves and discontinuities (Tsurutani et al., 1988a; 1994). The plasma temperatures are quite low. The smooth fields allow bi-directional flow of electrons and ions which have been observed (Gosling et al., 1987; Marsden et al., 1987). Galvin et al. have emphasized the existence of an anomalous region from 0630-0830 UT just upstream of the magnetic cloud. This interval is characterized by higher density and temperature plasma, and enhanced He^{++}/H^+ values. There is also enhanced Fe (at temperatures from 1.8×10^6 K to $~3.5 \times 10^6$ K) in this region (not shown). The region is also bounded by magnetic field discontinuities at ~0630 and ~0830 UT. It is speculated that this plasma is the remnants of the bright loops of the CME. Such structures upstream of magnetic clouds are present 20-40% of the time at 1 AU.

Magnetic Cloud Driven Storms

A classic example of a magnetic storm driven by a magnetic cloud is shown in Figure 5. The forward shock is denoted by an "S" and a vertical dashed line in the Figure, and the Stint Of the magnetic cloud by a second dashed vertical line. The preshocked solar wind speed is ~400 km s^{-1} and the post shock speed ~550 km s-'. The magnetic field increased from ~6 nT to ~22 nT across

the shock. Because $B_z \sim 0$ in the sheath, there is no increased ring current activity associated with the sheath fields.

The plasma density increases from 5 cm^{-3} to >40 cm^{-3} across the shock. Because of this density (and velocity) increase across the. shock, the increased ram pressure exerted on the earth's magnetosphere, ρV_{sw}^2, causes a sudden compression of the magnetosphere and a positive jump in the horizontal component of the equatorial-region field. A positive jump in D_{ST} is noted at the time of the shock. This is a sudden impulse (SI) event. Since the SI is eventually followed by a storm main phase, it is called a storm sudden commencement or SSC (however, it has been argued [Joselyn and Tsurutani, 1990; Gonzalez, cl al., 1992] that this latter term is an artificial label because the physics of a SI [ram pressure increase] is independent of whether it is followed by a storm main phase or not).

The storm main phase occurs in near-coincidence with the sharp southward turning of the IMF at the magnetic cloud boundary. The delay is ~1 hour (Gonzalez et al., 1989). The storm main phase (decrease in D_{ST}) development is rapid and the decrease monotonic. In the example of Fig. 5, the peak D_{ST} value of -239 nT is reached ~two hours after the peak B_S value of ~-30 nT.

It should be noted that the southward turning of the IMF was abrupt, and after the maximum B_S was reached, B_S was constant for several hours and they slowly and smoothly rotated [0 a northward direction.

The storm recovery phase is initiated by a gradual turning of the IMF to a northward direction from 1600 UT day 354 to 1400 UT day 355. The recovery starts as the field becomes less southward, is smooth and the I/c time scale is a fraction of a day. Further discussions on the configuration and evolution of magnetic clouds and their geoeffectiveness can be found in a companion paper by Farrugia et al. (this issue).

Magnetic Storms Caused by Sheath Fields

There are numerous mechanisms that lead to southward component fields in the sheath. A number of these are indicated schematically in Figure 6.

Two of the mechanisms lead to the intensification of magnetic fields, independent of whether they are oriented in a northward or a southward direction. They are shock compression b), discussed

previously, and (1) draping. 111 the former mechanism, the shock compresses both the magnetic field and plasm. In the latter mechanism (Midgley and Davis, 1963; Zwan and wolf. 1 976), draping of magnetic fields around a large object (in this case, the solar ejecta) leads to a squeezing of plasma out the ends of magnetic flux tubes. Although the dynamic pressure ($B^2/8\pi - t \sum N_i kT_i$) is maintained across the whole sheath, draping leads to lower beta plasmas and thus higher field strengths. The so-called "plasma depletion layer adjacent to the earth's magnetopause is a simple consequence of this effect, and should be present to some degree near the sheath stagnation points at all large objects where magnetic draping occurs (Farrugia et al., this issue).

Figure 7 illustrates the generation of magnetic storms by the shock compression mechanism. From day 245 until the shock on day 248, the B_z value was fluctuating, but generally had a southward component. There is corresponding auroral electrojet (AE) activity as well as ring current (D_{ST}) activity present. D_{ST} was ~ -30 nT from day 245 until the middle of day 247, and ~ -50 nT thereon until the shock. These D_{ST} values are relatively constant with little or no sign of the classic main phase/recovery phase signatures.

There is a short duration increase (small spike) in D_{ST} at and just after the shock due to solar wind ram pressure effects. This Sudden Impulse is the totality of the storm initial phase.

The B_z values in the sheath region behind the shock are fluctuating, but primarily directed southward from the shock until 1600 UT day 250. The peak B_S value of - -20 nT is reached at ~1200 UT day 249 and the peak Ds, of -280 nT several 110111's later. The mechanism for the southward component magnetic fields causing this storm are shock compression plus possible effects of draping.

Whether intense interplanetary fields are those of the sheath or the ejecta, the energy injection mechanism into the magnetosphere is the same. This is schematically shown in Figure 8. Interconnection of interplanetary fields and magnetospheric dayside fields leads to the enhanced reconnection of fields on the nightside with the concomitant deep injection of plasmasheet plasma in the nightside. The latter leads to the formation of the storm-time ring current. In general, the IMF structures leading to great ($D_{ST} < - 250$ nT) and intense ($D_{ST} < -100$ nT) magnetic storms have features similar to the examples shown. The IMF B_S is intense and has a long duration. Major B_z fluctuations are about 0 nT not present. Gonzalez and Tsurutani (1987) have empirically found that interplanetary events with $E_{dawn-dusk} > 5$ mV/m (approximately $B_S > 10$ nT) with T > 3 hours lead to intense ($D_{ST} < -100$ nT) magnetic storms.

6

In Tables 1 and 2 we give the causal connection between shocks/solar ejecta and storms of various levels of strength where we have defined the latter as follows: big: $D_{ST} < -200$ nT, intense: (-200 nT $\leq D_{ST} < -100$ nT, moderate: -100 nT $\leq D_{ST} < -50$ nT and small: -50 nT $\leq D_{ST} < -30$ nT magnetic storms. These come from prior work of the authors and from Gosling et al. (1991). Gosling et al. (1991) used Kp indices, and we have indicated the approximate D_{ST} values corresponding to these values. The Tables show that big storms have a 90% correspondence with fast solar eject events (with shocks), while small storms have only a 24% correspondence with fast solar ejecta.

Table 1 indicates that solar ejecta led by shocks do not always cause intense ($D_{ST} \leq -100$ nT) magnetic storms. Studies using the ISEE-3 1978-19-/9 data indicate that only one out of every six solar ejecta ([7$\%$) are geoeffective in causing intense storms (Tsurutani et al., 1988 b). From 57 fast solar ejecta events, it was found that some of the events did not have substantial B_s, others had large B_s values, but were highly fluctuating (about $B_z = 0$ nT) in time. The important point is that they did not have $B_s > 10$ nT for $T > 3$ hours.

Table 3 gives the statistics for moderate magnetic storms. At these lower levels of storm intensity, one notes that the interplanetary causes are much more diverse. There are many mechanisms responsible for the causative B_s values. One such case (Alfvén fluctuations) were indicated in Figure 7 for the geomagnetic activity in the preshock interval. The general southward component (possibly intensified by the Russell-McPherron [1973] mechanism) and fluctuating B_z led to $D_{ST} \sim -50$ nT.

Viscous Interaction

The earth's magnetopause can absorb solar wind energy through the fluid analogy of a viscous interaction (Axford and Hines, 1961). More specifically, mechanisms such as the Kelvin Helmholtz instability (Parker, 1958, Tamao, 1965; Chen and Hasegawa, 1974; Southwood, 1968, 1974) or magnetosheath cross-field diffusion due to magnetopause boundary layer waves (Tsurutani and Thorne, 1982; Gendrin, 1983; Thorne and Tsurutani, 1991), are possible ways to inject solar wind energy into the magnetosphere.

An upper limit of the efficiency of solar wind energy access to the magnetosphere has been explored by examining intervals where the northern IMF component $B_n > 10$ nT and '1' > 3 hours. These interplanetary conditions allow reconnection between the IMF and terrestrial field tailward

of the cusp (e. g., Dungey, 1963; Russell, 1972) hence justifying the statement that this is an upper limit calculation. The actual efficiency value might be lower. Without going through the (reasonably simple) details of the calculations, the conclusion is that -1 to 4×10^{-3} of the solar wind ram energy is converted to magnetospheric energy in the fol'in of auroral particles energy, Joule heating, or ring current particle energy (Tsurutani and Gonzalez, J 995b).

The efficiency of solar wind energy injection during magnetic reconnection events such as substorms and intense storms is 5- 10% (Weiss et al., 1992, Gonzalez et al., 1989, respectively). The intercomparison of these numbers indicates that viscous interaction appears to be not IllOIL' than 1/100th to 1/30 as efficient than magnetic reconnection. The highest solar wind speed event ever detected ($V_{sw} > 1500$ km s-', August, J 972) has also been studied for this cl'feet. The efficiency of viscous interaction was found to have approximately the same value for this event as well (Tsurutani et al., 1 99?).

It should be noted that northward B_z intervals satisfying the $B_z <-10$ nT and '1'> 3 hours criteria are often found to be a portion of a magnetic cloud. Thus, since magnetic clouds often have south and then northward magnetic field orientations (or vice versa), clouds often cause magnetic storms followed by geomagnetic quiet (or vice versa).

Descending Phase of the Solar Cycle

In contrast to solar maximum, where coronal holes are not very important during this phase of the solar cycle, the interplanetary medium is dominated by the effects of large coronal holes at the sun. The polar coronal holes extend from the polar regions down to the equator and sometimes even far past the equator (see Jackson, this issue). Coronal holes are low temperature regions above the sun, observed in soft x-rays (Timothy et al, 1975). They are areas of open magnetic field lines. Ulysses has shown that holes are regions of fast streams with velocities of 750-800 km s^{-1} (I 'hillips et al., 1994) and are dominated by large amplitude Alfvén waves (Tsurutani et al., 1994, 1996; Balogh et al., 1995; Smith et al., 1995a, b). The Alfvén waves are continuously present in the high velocity streams.

During the descending phase of the solar cycle, when the holes migrate down to lower latitude as "fingers", the streams cremating from (11C holes "corotate" at -27 day intervals (as seen at the Earth), and thus plasma from these streams impinge on the Earth's magnetosphere at periodic intervals and cause recurrent geomagnetic storms (Burlaga and Lepping, 1977; Sheeley et al., 1976, 1977; Burlaga et al., 1978).

High speed streams emanating from coronal holes can create intense magnetic fields if the streams interact with streams of lower speeds (Belcher and Davis, 1971; Pizzo, 1985). A schematic of such an interaction is given in Figure 9. The magnetic fields of the slower speed stream are more curved due to the low speeds, and the fields of the higher speed stream are more radial because of the higher speeds. The stream-stream interface (IF) is the boundary between the slow stream and fast stream plasmas and fields. Significant angular deflections in velocity can occur at or near this region (see Pizzo, 1985).

Antisunward of the IF are the compressed and accelerated slower speed plasma and fields. Behind the IF are the compressed and decelerated high speed stream plasma and fields. At large heliospheric distances (> 1.5 AU), where these corotating structures are well developed, they are bounded by fast forward (FS) and fast reverse (RS) shocks. This overall structure was first found in the Pioneer 10 and 11 data and were named Corotating Interaction Regions (CIRs) by Smith and Wolf (1976). See also Burlaga et al. (1985). As far as geomagnetic storms are concerned, the important feature of CIRs is that they are characterized by intense magnetic fields. The intensities can reach ~30nT.

At 1 AU, CIRs are not fully developed. They almost never have forward shocks (this can and has been used as a reasonably reliable identifying feature) and usually do not have reverse shocks (~80% of the time). We therefore call these proto-CIRs (PCIR) in this paper.

An example of a PCIR and its consequential magnetic storm activity is shown in Figure 10. This event is typical of the events studied for the 1973- 1975 epoch where two corotating streams (from two coronal holes) per solar cycle dominated interplanetary activity.

The unusually high plasma densities of > $50 \, cm^{-3}$ at the beginning of day 25 is intrinsic to the slow solar wind near the heliospheric current sheet (HCS), the region separating the north and south hemisphere heliospheric magnetic fields. This high density plasma has been called the HCS plasma sheet by Winterhalter et al. (1995). (However, Lepping, et al. (1996) note that this plasmasheet may not always be present). The HCS is identified by a reversal in the Parker spiral direction by ~180° or a simultaneous reversal in the signs of both B_x and B_y. Such a reversal can be noted at ~2200 UT day 24.

The high density plasma of the HCS plasma sheet causes the "initial phase" of the magnetic storm noted in the bottom panel. Note that this "phase" Of the storm is caused by interplanetary

conditions totally unlike those during solar maximum. Here the high densities are associated with a low velocity stream ($V_{SW} < 400$ km s^{-1}). Since the PCIRs typically do not have forward shocks at 1 AU, there will typically be lack of a sudden impulse associated with this type of a storm.

The magnetic field of the PCIR increases gradually from about 0000 UT until 2000 UT day 25. A maximum value of ~25 nT is present from 1200 to 2000 UT. In this particular case, the PCIR is terminated by a reverse shock.

The PCIR is responsible for the main phase of the magnetic storm. The reverse **Shock.** across which the field decreases dramatically, leads to the start of the recovery phase of the magnetic storm with a delay of about 1]1OLII. W C note, however, that the storm main phase is somewhat irregular in profile and the peak intensity is only 1) s, ~ -70 nT (this is on the upper end of storm strength distribution during this phase of the solar cycle). The cause of this is in the character of B_z within the PCIR. B_z is highly fluctuating throughout the interval. '1' h e r e may be a net southward component within the PCIR, but this is accompanied by a much larger f l u c t u a t i o n amplitude.

Why are such fluctuations present? One possible answer is schematically shown in Figure 9. If B_z fluctuations (Alfvén waves) are present in the high speed stream proper, then the deceleration and compress ion due to passage through the reverse shock could lead to amplification of such oscillations. Ulysses results (Tsurutani et al., 1995a) are consistent with such a scenario.

Figure 11 shows the geomagnetic activity during 1974 when there were two corotating streams (per 27 day solar rotation) present. The 3 storms where 1)s, < -100 nT were caused by fields associated with solar ejecta events and not by the corotating streams. Thu s, the corotating streams are far less geoeffective in creating intense or moderate magnetic storms.

A summary of the geoeffectiveness of PCIRs is given in Table 4. This was derived from a subset of the 1974 dots set, Similar studies have been performed on the 1973 and 1975 data, with similar results.

Maximum Geomagnetic Activity During Solar Maximum or Solar Minimum?

Although it is clear that there are far more large D_{ST} events during solar maximum than during solar minimum, the same cannot be said for auroral zone (AE) activity. For the period 1973-1975, the annual AE average (of the 2.5 min values) were: 247, 283 and 224 nT, respectively. For 1979-

1981, the annual AE values were 221, 180 and 237 nT. The 283 nT value for 1974 was larger than any of the solar maximum years.

The causes for this effect can be found in Figure 11. After each magnetic storm interval (sharp D_{ST} decrease), there are prolonged intervals of intense AE. These AE intensifications are directly correlated with the slow recovery of D_{ST}. In most of the events shown in the Figure, the D_{ST} index takes 10-20 days to recover to near-background values.

Figure 12 illustrates a four day period of one of these storm recovery intervals. D_{ST} fluctuates at a value near -25 nT for the entire period with little or no sign of recovery. An intercomparison with the AE index indicates that there is a one-to-one relationship between AE increases and D_{ST} decreases. Thus one interpretation of this observation is that substorms (AE increases) are injecting fresh particles into the outer radiation belts, preventing the ring current from reaching quiet day values. However, it should be noted that plasmasheet current intensifications or earthward motions of the latter could cause such effects on the D_{ST} index as well. This problem will be investigated in the near future.

The cause of the continuous substorms in Figure 12 are the large amplitude B_z fluctuations in the IMF. Although the average B_z value is near zero, the large amplitude fluctuations provide very large B_s intervals and concomitant substorms through the reconnection process. The IMF fluctuations have been examined and have been shown to be Alfvén waves propagating outward from the sun in these coronal hole streams. The fluctuations are more or less continuous and the southward components of the larger period waves cause High Intensity Long Duration Continuous AE Activity (HILDCAAs) (Tsurutani and Gonzalez, 1987; Tsurutani et al, 1990).

Axford, W. I. and C. O. Hines, A unifying theory of high-latitude geophysical phenomena and geomagnetic storms, Can. J. Phys., 39, 1433, 196

Balogh, A., E. J. Smith, B. T. Tsurutani, D. J. Southwood, R. J. Forsyth, and T. S. Horbury, The heliospheric magnetic field over the south polar region of the sun, Science, 268, 007, 995

Bravo, S. and J. A. L. Cruz-Abeyo, The spatial relation between active regions and coronal holes, and the occurrence of geomagnetic storms, Chapman Conference on Magnetic Storms, Pasadena, California, February 12-6, 1996.

Belcher, J. W. and L. Davis, Jr., Large amplitude A fvén waves in the interplanetary medium, 2, J. Geophys. Res., 76, 3534, 971.

Burlaga, L. F. and R. P. Lepping, The causes of recurrent geomagnetic storms, Planet. Space Phys., 1151, 1977

Burlaga, L. F., K. W. Behannon, S. F. Hansen, G. W. Pneuman and W. C. Feldman, Sources of magnetic fields in recurrent interplanetary streams, J. Geophys. Res., 83, 4177, 1978.

Burlaga, L. F., F. Sittler, F. Mariani, and R. Schwenn, Magnetic loop behind an interplanetary shock: Voyager, Helios and IMP-8 observations, J. Geophys. Res., 86, 6673, 98

Burlaga, F. V. Pizzo, A. azarus and P. Gazis, Stream dynamics between 1 AU and 2 AU: A comparison of observations and theory, J. Geophys. Res., 90, 7317, 1985.

Burlaga, L. F., K. W. Behannon, and L. W. Klein, Compound streams, magnetic clouds and major geomagnetic storms, J. Geophys. Res., 92, 5725, 1987.

Burlaga, L.F., R. P. Lepping and J. Jones, in Physics of Flux Ropes, ed. C. T. Russel ; R Priest and L. C. Lee, AGU Monograph 58, Wash. D.C., 373, 1990.

Chen, L. and A. Hasegawa, A theory of long-period magnetic pulsations, 1), Study state excitation of field-line resonances, J. Geophys. Res., 79, 024, 974

Choe, G. S., N. LaBelle-Hamer, B. T. Tsurutani and L. C. Lee, Identification of a driver gas boundary layer, EOS, 73, 485, 1992.

Dungey, J. W., The structure of the exosphere on adventures in velocity space, ii Geophys., The Earths Env., edited by C. DeWitt and J Hieblot, 505, Gorden and Breach, N.Y., 963.

Farrugia, C. J., F. Burlaga, V. A. Osherovich, I. G. Richardson, M. P. Freeman, R. P. Lepping and A J. Lazarus, A study of an expanding interplanetary magnetic cloud and its interaction with the Earth's magnetosphere: the interplanetary aspect, J. Geophys. Res., 98, 7621, 1993a.

Farrugia, C. J., G. Richardson, L. F. Burlaga, R. P. Lepping and V. A. Osherovich, Simultaneous observations of solar MeV particles in a magnetic cloud and in the earth's

northern tail lobe: Implications for the global field line topologies of a magnetic cloud and for the entry of solar particles into the magnetosphere during cloud passage, J. Geophys. Res. , 98, 15497, 1993b.

Farrugia, C. J., V. A. Osherovich and 1,. F. Burlaga, Magnetic flux rope versus the spheromak as models for interplanetary magnetic clouds, J. Geophys. Res., 100, 12293, 1995.

Farrugia, C. J., L. F. Burlaga and R. 1', Leppping, Magnetic clouds and the quiet-stem effect at earth, submitted to Magnetic Storms, edited by B. 'I'. Tsurutani, W. D. Gonzalez and Y. Kamide, AGU Monograph, Wash. D.C., 1996.

Galvin, A. B., F. M. Ipavich, G, Gloeckler, 1). Hovestadt, S, J, Bame, B. Kleckler, M. Scholer and B. '1'. Tsurutani, Solar wind ion charge st at us preceding a driver plasma, J. Geophys. Res., 92, 12069, 1987.

Gendrin, R., Magnetic turbulence and diffusion processes in the magnetopause boundary layer, Geophys. Res. Lett., 769, 1983.

Gold, T., Magnetic storms, Space Sci. Rev., 1, 100," 1962.

Gonzalez, W. 1). and B. "I'. Tsurutani, Criteria of interplanetary parameters causing intense magnetic storms (1)s., <- I 00 nT), Planet. Space Sci., 35,1101, 1987.

Gonzalez, W. 1)., B. '1'. Tsurutani, A.L.C. Gonzalez, E. J. Smith, F. Tang, and S.-I. Akasofu, Solar wind magnetosphere coupling during intense magnetic storms (1978- 1979), J. Geophys. Res., 94, 8835, 1989.

Gonzalez, W.])., , A. 1.. Clua de Gonzalez, O.Mendes, Jr., and B. T. Tsurutani, Difficul ties in defining stem sudden commencements, EOS, Trans. Amer. Geophys. Un., 73,180, 1992.

Gonzalez, W, I)., B. '1'. Tsurutani, P. S. McIntosh, and A, 1.. Clua de Gonzalez, Coronal hole - net ive region - current sheet (CHARC 'S) association with intense interplanetary and geomagnetic activity, Geophys. Res. Lett., submitted, 1996.

Gosling, J. T., D. N. Baker, S. J. Bame, W. C. Feldman and R. D. Zwickl, Bi-directional solar wind electron heat flux events, J. Geophys. Res., 92,8519,1987.

Gosling, J. '1'., S., J. Bame, D. J. McComas, and J. L. Phillips, Coronal mass ejections and large geomagnetic storms, Geophys. Res. Lett., 127, 901, 1990.

Gosling, J. '1'., D.J.McComas, J. 1. Phillips and S. J. Bame, Geomagnetic activity associated with Earth passage of interplanetary shock disturbances and coronal mass ejections. J. Geophys. Res., 96, 7831, 1991.

Ivanov, K. G., A. F. Harschiladze, E. G. Eroshenko, and V. A. Styazhkin, Configuration, structure and dynamics of magnetic clouds from solar flares in light of measurements on board Vega 1 and Vega 2 in Jan. -Feb. 1986, Solar Phys., 120, 407, 1989.

Jackson, B. V., Heliospheric observations of solar disturbances and their potential role in the origin of storms, this issue.

Joselyn, J. A. and B. T. Tsurutani, Geomagnetic sudden impulses and storm sudden commencements , EOS, 7LL808 1990.

Klein, L. W. and L. F. Burlaga, Interplanetary magnetic clouds at 1 A, J. Geophys. Res., 87, 613, 1982.

Lepping, R. P., J. A. Jones, L. F. Burlaga, Magnetic field structure of interplanetary magnetic clouds at 1 AU, J. Geophys. Res., 95, 1195"1, 1990.

Lepping, R. P., A. Szabo, M. P'credo, and A. Campbell, Summary of heliospheric current and plasma sheet studies: WIND observations, Proc. Sol. Wind B, ed. D. J. McComas, 1996.

McComas, D. J., J. "P'. Gosling, S. J. Bame, E. J. Smith, and 11. V. Cane, A test of magnetic field draping induced B_z perturbations ahead of fast coronal mass ejecta, J. Geophys. Res., 94, 1465, 1989.

Marsden, R. G., T. R. Sanderson, C. Tranquille and K.-P'. Wenzel, ISEE-3 observations of IOw-energy proton bi-directional events and their relation to isolated interplanetary magnetic structures, J. Geophys. Res., 92, 11 0()9, 1987.

Midgley, J. E. and L. Davis, Jr., Calculation by a moment technique of the perturbation of the geomagnetic field by the solar wind, J. Geophys. Res., 68, 51 11, 1963.

Odstrcil, 1)., Numerical simulation of interplanetary plasma clouds propagating along the heliospheric plasma sheet, Astrophys. Lett. Comm. in press. 1996.

Parker, E. N. Interaction of solar wind with the geomagnetic field, Phys. Fluids. 1, 1‛/ 1, 1958.

Phillips, J. 1,., A. Balogh, S. J. Bame, et al]., Ulysses at 50° south: constant immersion in the high-sped solar wind, Geophys. Res. Lett.), 2 1, 1105, 1994.

Philips, J. 1,., S. J. Bame, W. C. Feldman, B. E. Goldstein, J. T. Gosling, C. M. Hammond, D. J. McComas, M. Neugebauer, E. E. Scime and S. "P'. Suess, Ulysses solar wind plasma observations at high southerly latitudes, Science, 268, 1030, 1995.

Pizzo, V. J., Interplanetary shocks on large scale: A retrospective on the last decade's theoretical efforts, in Collisionless Shocks in the Heliosphere. Review of Current Research, ed. by B. T. "P'Sill'Lltalli and R. G. Stone, Geophys. Mon. Series, 35, 51, Wash D.C., 1985.

Russell, C. T., The configuration of the magnetosphere, in Critical Prob Magnet. Phys., edited by E. R. Dyer, 1, Nat. Acad. Sci., Wash. D.C., 1972.

Russell, C. 1'. And R. 1. McPherron, Semiannual variation of geomagnetic activity,_ .1. Geophys. Res., 78, 92, 1973.

Sheeley, N. R., Jr., J. W. Harvey, and W. C. Feldman, Coronal holes, solar wind streams and recurrent geomagnetic disturbances, 1973-1 9‛/6, Sol. Phys., 49, 271, 1976.

Sheeley, N. R. Jr., J. R. Asbridge, S. J. Bame and J. W. Harvey, A pictoral comparison of interplanetary magnetic field polarity, solar wind speed, and geomagnetic disturbances index during the sunspot cycle, Sol. Phys., 52, 485, 1 9‛/7.

Smith, E.J. and J. W. Wolfe, Observations of interaction regions and corotating shocks between one and five AU: Pioneers 10 and 11, Geophys. Res. Lett., 3, 137, 1 976.

Smith, E. J., M. Neugebauer and B. T. Tsurutani, Ulysses observations of latitudinal gradients in the heliospheric magnetic field: Radial component and variances, Space Sci. Rev., 72, 165, 199s:1.

Smith, E. J., A, Balogh, M. Neugebauer, and 1). McComas, Ulysses observations of Alfvén waves in the southward northern solar hemisphere, Geophys. Res. Lett., 22, 3381, 1995b.

Southwood, I). J., The hydromagnetic stability of the magnetospheric boundary, Planet. Space Sci., 16, 587, 1968.

Southwood, D. J., Some features of field-line resonance in the magnetosphere, Planet. Space Sci., 22, 483, 1974.

Tamao, T., Transmission and coupling resonance of hydromagnetic disturbances in non-uniform Earth's magnetosphere, Sci. Rep. Tohaku Univ. Ser., 5, 17, 43, 1965.

Thorne, R, M. and B. T. Tsurutani, Wave-part icle interactions in the magnetopause boundary layer, in Physics of Space Plasmas (1 990), ed. by T. Chang, et al. sci Publ. Inc., Cambridge, MA, -J(), 119, 1991.

Timothy, A. F., A. S. Krieger and (i. S. Vaiana, The structure and evolution of coronal holes, Sol. Phys. 42, 13s, 1975.

'J'sill'll[alli, B. T. and R. M. 'l'home, Diffusion processes in the magnetopause boundary layer, Geophys. Res. Lett., 9, 1247, 1982.

Tsurutani, B. T., C. T. Russell, J. H. King, R. 1). Zwickl, and R. P. Lin, A kinky heliospheric current sheet: Causes of the CDAW6 substorms, Geophys. Res. Lett., 11, 339, 1984.

Tsurutani, B. T. and W. I). Gonzalez, The cause of high intensity long-duration continuous AE activity (1 Ill DCAAs): Interplanetary Alfvén waves trains, Planet. Space Sci., 35, 405, 1987.

Tsurutani, B. T., W. 1). Gonzalez, F. Tang, S.-1. Akasofu, and E. J. Smith, Origin of interplanetary southward magnetic fields responsible for major magnetic Stol'ills near solar maximum (1978- 1979), J. Geophys. Res., 93, 8519, 1988a.

Tsurutani, B. 'l '., B. E. Goldstein, W. I). Gonzalez, and F. Tang, Comment on "A new method of forecasting geomagnetic activity and proton s]1owc1's", by A. Hewish and P. J. Duffet-Smith, Planet. Space Sci., 36, 205, 1988b.

Tsurutani, B. 'l'., 'l'. Gould, B. E. Goldstein, W. 1). Gonzalez, and M. Sugiura, Interplanetary Alfvén waves and auroral (substorm) activity: 1 MP-8, J, Geophys. Res., 95, 2241, 1990.

Tsurutani, B. T., W. I). Gonzalez, F. Tang, 'l'. 'J'. 1 .ee, M. Okada, and]). Park, Reply to L.J. Lanzerotti: Solar wind ram pressure corrections and an estimation of the efficiency of viscous interaction, Geophys. Res. Lett., 1 9, 1 993, 1 992.

Tsurutani, B. T., C. M. Ho, E. J. Smith, M, Neugebauer, B. E. Goldstein, J. S. Mok, J. K. Arballo, A. Balogh, D. J. Southwood and W. C. Feldman, The relationship between interplanetary discontinuities and Alfvén waves: Ulysses observations, Geophys. Res. Lett., 21, 2267, 1994.

Tsurutani, B. 'T'. and W. D. Gonzalez, The future of geomagnetic stem predictions: Implications from recent polar and interplanetary observations, J. Atmos. Terr. Phys., 57, i 369. 1995: 1.

Tsurutani, B. 'T'. and W. D. Gonzalez, The efficiency 01' "vi scous interaction" between the solar wind and the magnetosphere during intense northward 1 M F events, Geophys. Res. Lett., 22, 663, 1995b.

Tsurutani, B. 'T'., C. M. Ho, J. K. Arballo, B. E. Goldstein, and A. Balogh, Large Amplitude IMF fluctuations in corotating interaction regions: Ulysses at midlatitudes, Geophys. Res. Lett, 22, 3397, 1995a.

Tsurutani, B. T., W. D. Gonzalez, A.L.C. Gonzalez, F. Tang, J. K. Arballo and M. Okada, Interplanetary original of geomagnetic activity in the declining phase of the solar cycle, J. Geophys. Res. 100, 21717, 19951).

Tsurutani, B. 'T'., B. E. Goldstein, C. M. Ho, M. Neugebauer, E. J. Smith, A Balogh and W. C. Feldman, Interplanetary discontinuities and Alfvén w a v e s at high heliographic latitudes: Ulysses, J. Geophys. Res., 101,] 1027, i 996.

Vandas, M., S. Fischer and A. Geranios, Spherical anti cylindrical models of magnetic clouds and their comparison with spacecraft data, Planet. Space Sci., 39, i 147, i 99 i.

Vandas, M., S. Fischer, P. Pelant and A. Geranios, Spheroidal models of magnetic clouds and their comparison with spacecraft measurement. J Geophys. Res., 98, 11467. 1993.

Weiss, 1,. A., P.H. Reiff, J. J. Moscs, and B. D. Moore, Energy Dissipation in substorms, Eur. Space Agency Spec. Publi., ESA-SP-335, 309, 1992.

Winterhalter, D., E. J, Smith, M. E. Burton, N. Murphy and D. J, McComas, The heliospheric plasma sheet, J. Geophys. Res., 99, 6667, 1994.

Zwan, B. J. and R. A. Wolf, Depletion of the solar wind plasma near a planetary boundary, J. Geophys. Res., 81, 1636, 1976.

FIGURE CAPTIONS

Figure 1. Regions of intense interplanetary magnetic fields during solar maximum. T_1 and T_2 are two types of satellite crossings of the interplanetary structure.

Figure 2. Types of solar ejecta magnetic fields.

Figure 3. An example of a coronal mass ejection as seen in a white light coronograph image taken during the Solar Maximum Mission (courtesy of A. Hundhausen).

Figure 4. An example of possible remnants of the "bright loops" region (of a CME) followed by a magnetic cloud (taken from Galvin et al., 198-/).

Figure **5.** A classical example of a magnetic storm driven by a magnetic cloud. The vertical dashed line labeled by a "S" indicates the presence of a fast forward shock. The vertical dashed line to the right indicates the start of the magnetic cloud.

Figure 6. Types of "sheath" magnetic field structures.

Figure 7. Example of a magnetic stem caused by shock compression 01 interplanetary B_S fields..

Figure 8. Schematic of interplanetary-magnetosphere coupling, showing the energy injection mechanism into the nightside magnetosphere.

Figure 9. Schematic of the formation of corotating interaction regions (C IRs) during the descending phase of the solar cycle. The compression of plasma and magnetic field fluctuations are also shown. Taken from Tsurutani et al. (1995a).

Figure 10. Example of a PCIR and associated geomagnetic activity, typical of 1973-1975. Taken from 'T'sill'lltmi et al. (1995b).

Figure 11. Geomagnetic activity indices for 1974.

Figure 12. An example of a recovery phase of a magnetic storm during a HILDCAA interval.

ISEE-3 (Aug 1978 - Dec 1979)

	No. of Events	Definition	Association with Shocks (56) (supermagnetosonic speed CMEs)
Intense storms	10	$D_{ST} < -100$ nT	80%
Modera e storms	40	-100 nT $\leq D_{ST} \leq -50^{\circ}$ nT	45%
Smal storms	62	-50 nT $\leq D_{ST} \leq -30$ nT	24%

Shocks and Magnetic Storms

15% followed by intense storms

35% followed by moderate storms

30% followed by smal storms

2% followed by no storms ($D_{ST} \geq -30$ nT)

Table 1

Aug 1978- Ott 1982


```
      109    62    129
```

Shocks   CMEs
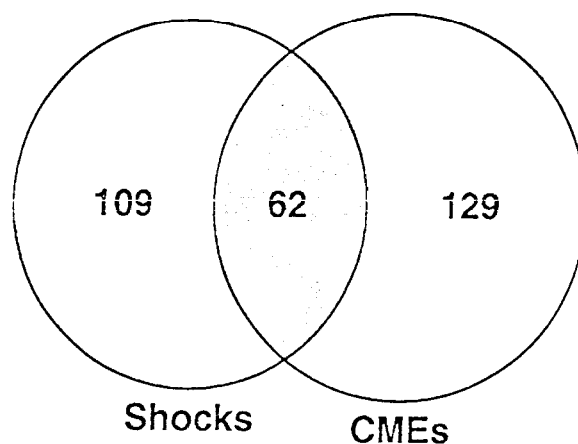
171 Shocks

191 CMES

62 Shocks with CMES

			Association	
			100% shocks	90% CMES
Big storms	$8 \leq K_p \leq 9$	$(D_{ST} \lesssim$ -200 nT)	100% shocks	90% CMES
Intense storms	$K_p = 7$	(-200 nT $\lesssim D_{ST} \lesssim$ -1OO nT)	80% shocks	80% CMES
Moderate storms	$5< K_p \leq 6$	(-100 nT $\lesssim D_{ST} \lesssim$ -50 nT)	40% shocks	40% CMES

Association

Shocks or CMES   15% lead to big or intense storms
                  40% lead to big, intense, or moderate storms

Shocks and CMES   50% lead to big or intense storms
                  70% lead to big, intense, or moderate storms

Table 2

Interplanetary Association of Moderate Storms
ISEE-3 (Aug 1978 - Dec 1979)

$$-100 \text{ nT} \leq D_{ST} \leq -50 \text{ nT}$$

40% Shocks

23% High-speed streams without shocks

17% High-Low speed stream interactions

10% NCDEs

10% Other (including Alfvénic fluctuations)

Table 3

Geoeffectiveness of Proto-CiRs
IMP-8   Days 1-241, 1974

We l-deve oped streams (V_{sw} = 600-850 km s^{-1})

ntense storms	(D_{ST} < -100 nT)	0%
Moderate storms	(-100 nT $\leq D_{ST}$ < -50 nT)	29%
Small storms	(-50 nT $\leq D_{ST}$ < -30 nT)	29%
Negligible storm activity	(-30 nT $\leq D_{ST}$)	41%

Table 4

FIGURE CAPTIONS

Figure . Regions of intense interplanetary magnetic fields during solar maximum. "J'₁ anti T₂ are two ypcs of satellite crossings of the interplanetary structure.

Figure 2. Types of solar ejecta magnetic fields.

Figure 3, An example of a coronal mass ejection as seen in a white light chronograph image taken during the Solar Maximum Mission (courtesy of A. Hundhausen).

Figure 4. An example of possible remnants of the "bright loops" region (of a CME) followed by a magnetic cloud (taken from Galvin et al., 1987).

Figure 5. A classical example of a magnetic storm driven by a magnetic cloud. The vertical dashed line labeled by a "S" indicates the presence of a fast forward shock. The vertical dashed line to the right indicates the start of the magnetic cloud.

Figure 6. Types of "sheath" magnetic field structures.

Figure 7. Example of a magnetic storm caused by shock compression of interplanetary B_s fields..

Figure 8. Schematic of interplanetary-magnetosphere coupling, showing the energy injection mechanism into the nightside magnetosphere.

Figure 9. Schematic of the formation of corotating interaction regions (CIRs) during the descending phase of the solar cycle. The compression of plasma and magnetic field fluctuations arc also shown. Taken from Tsurutani et al. (1995a).

Figure JO. Example of a PCIR and associated geomagnetic activity, typical of 1973-1975. Taken from Tsurutani et al. (1995 b).

Figure 1 i. Geomagnetic activity indices for 1974.

Figure 12. An example of a recover-y phase of a magnetic storm during a HILDCAA intervai.

Solar Maximum: Types of Large B Fields

T1: Crossing at the center of the shock/magnetic cloud structure

T2: Crossing off-center of the shock/magnetic cloud structure (missing the driver gas)

Figure 1

Driver Gas Fields

a) **First version of**
   magnetic clouds
   Klein and Burlaga, **1982**
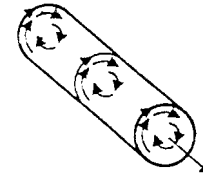
b) Fluxropes
   Burlaga **et al., 1990**

c) **Magnetic tongues**
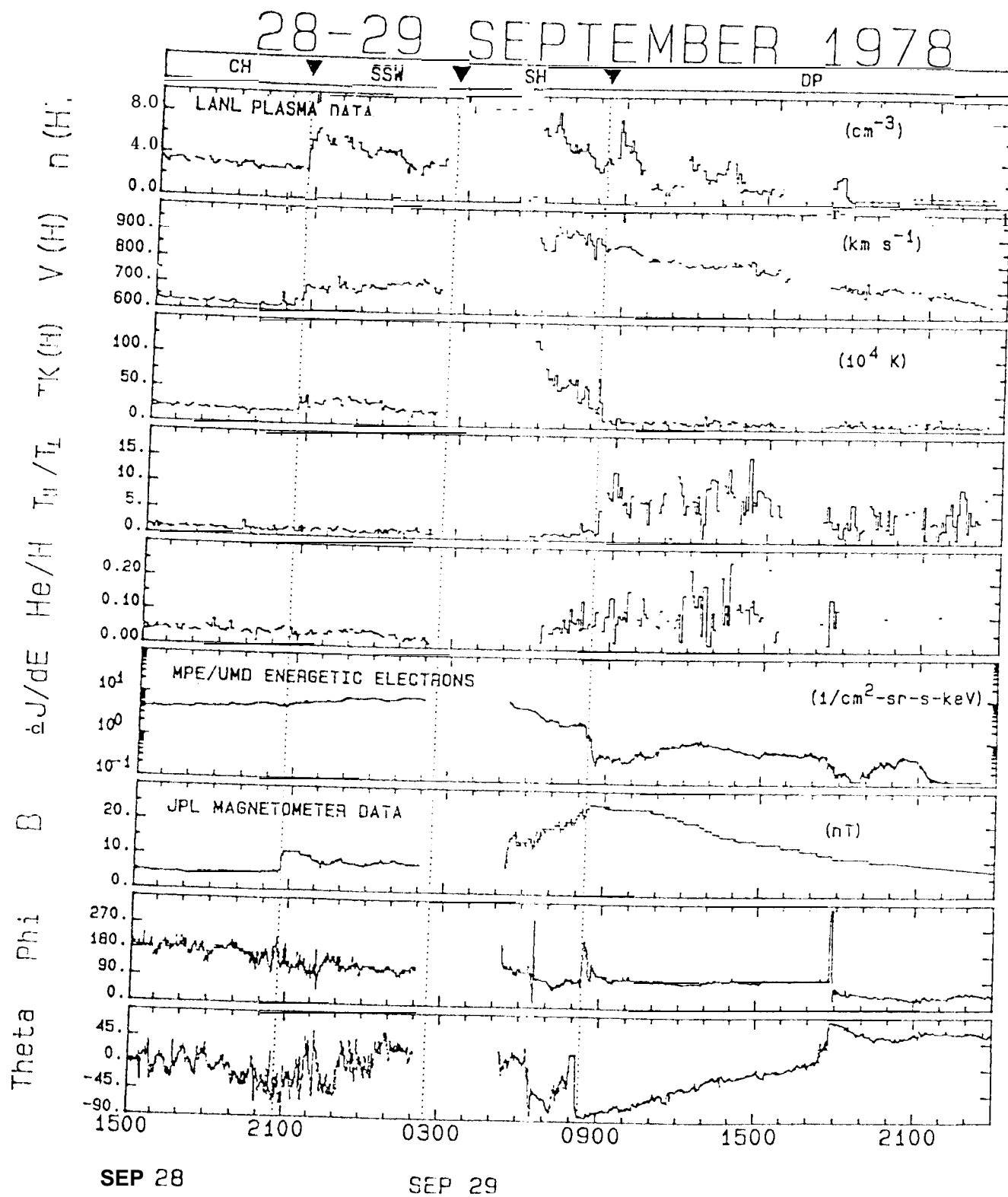   Gold, **1962**

Figure 2

18 Aug 1980: White Light

12:06 12:15

Source: High Altitude Observatory/Solar Maximum Mission Archives

13:34 HAO A-013
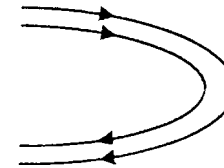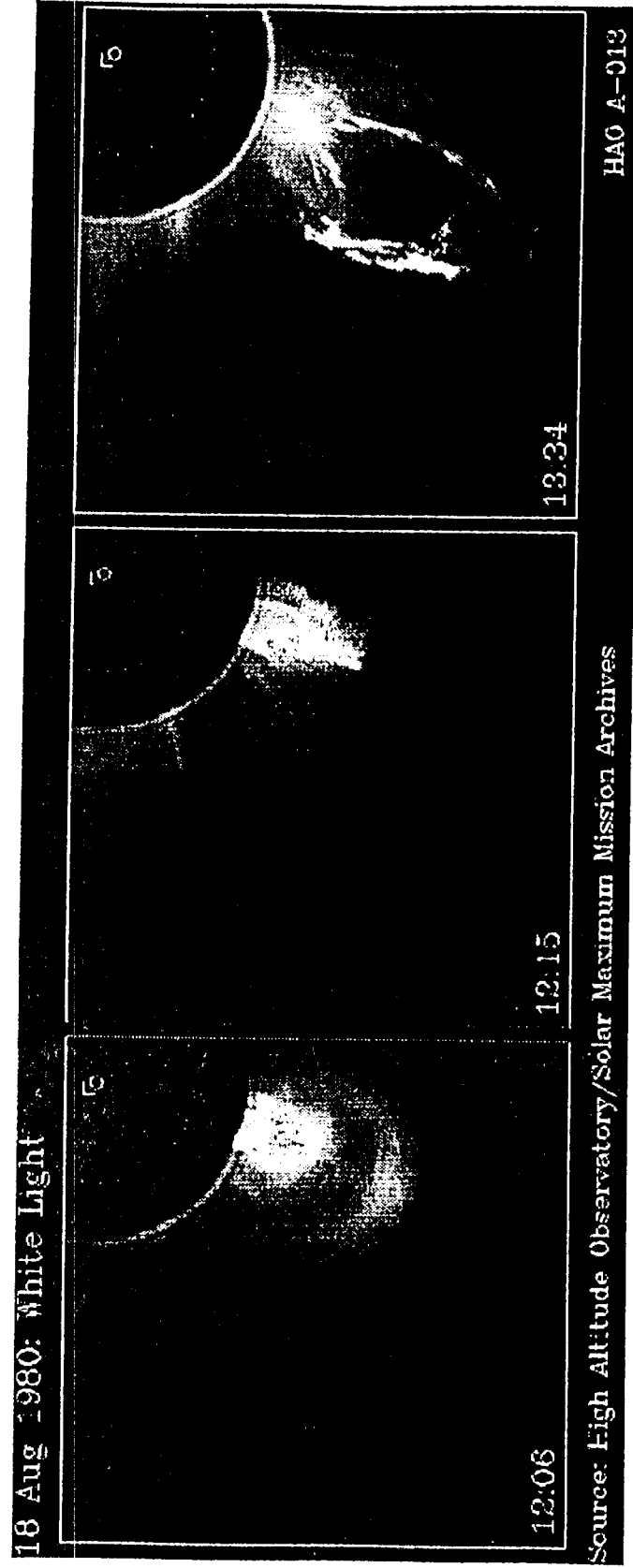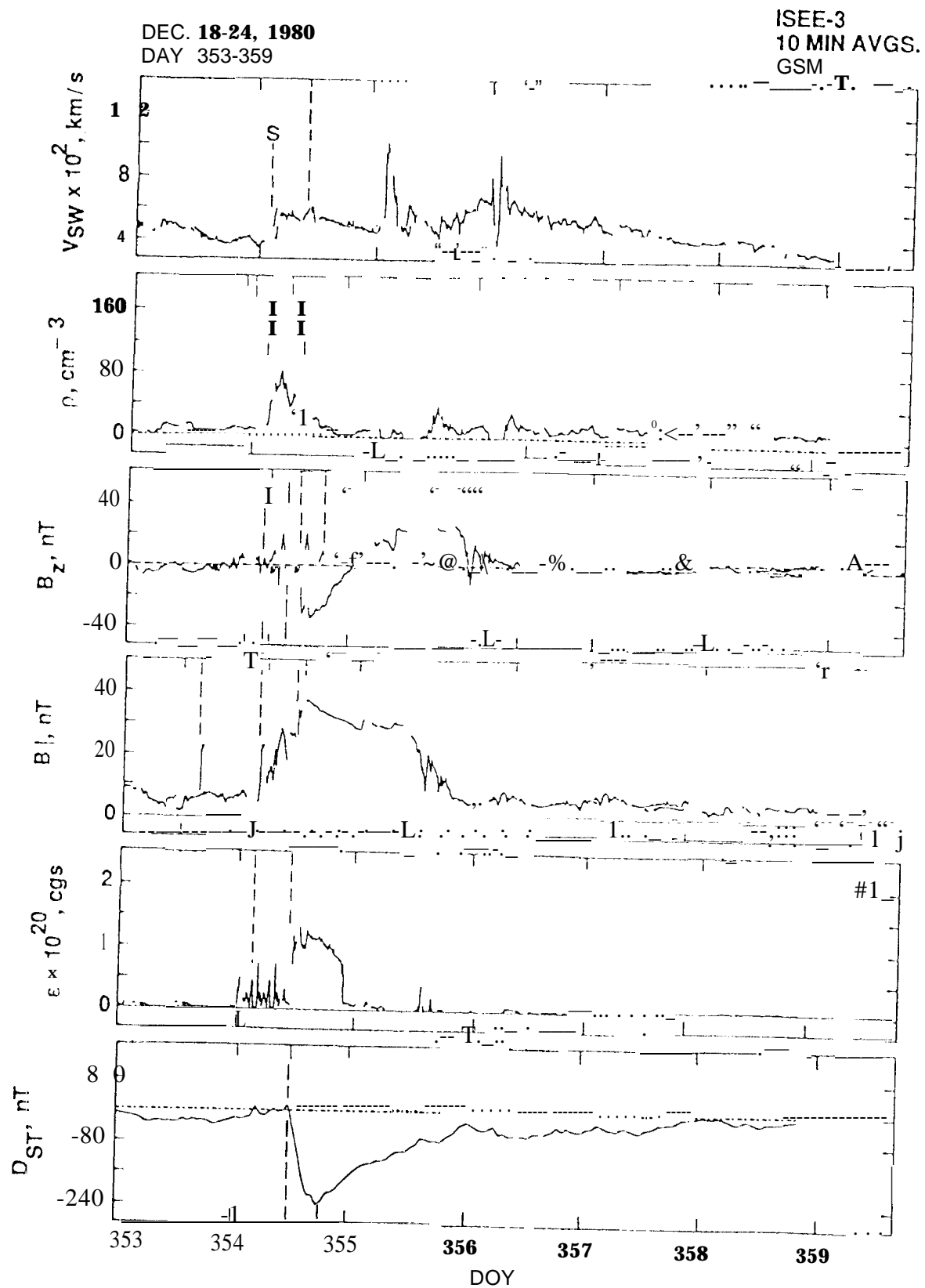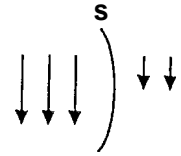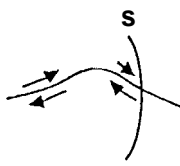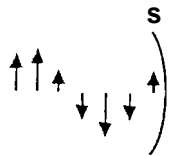
Figure 3

Figure 4

Figure 5
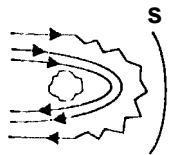
Sheath Fields
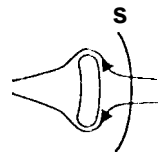
a) Shocked southward fields
   Tsurutani et al., 1988a
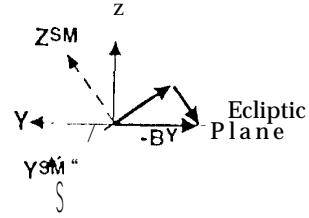
b) Heliospheric current sheets
   Tsurutani et al., 1984

c) Alfven waves and turbulence
   Tsurutani et al., 1995b

d) Draped magnetic fields
   Midgley and Davis, 1963
   Zwan and Wolf, 1976

e) Field draping
   McComas et al., 1989

f) Equinoctial By effect
   Russell and McPherron, 1973

g) Fast stream-HCS plasmasheet
   interaction
   Odstrcil, 1996

Figure 6

SEP. 02-12, 1982
DAY 245-255

ISEE-3
15 MIN AVGS.
GSM
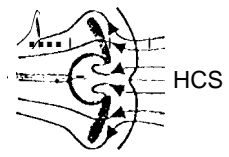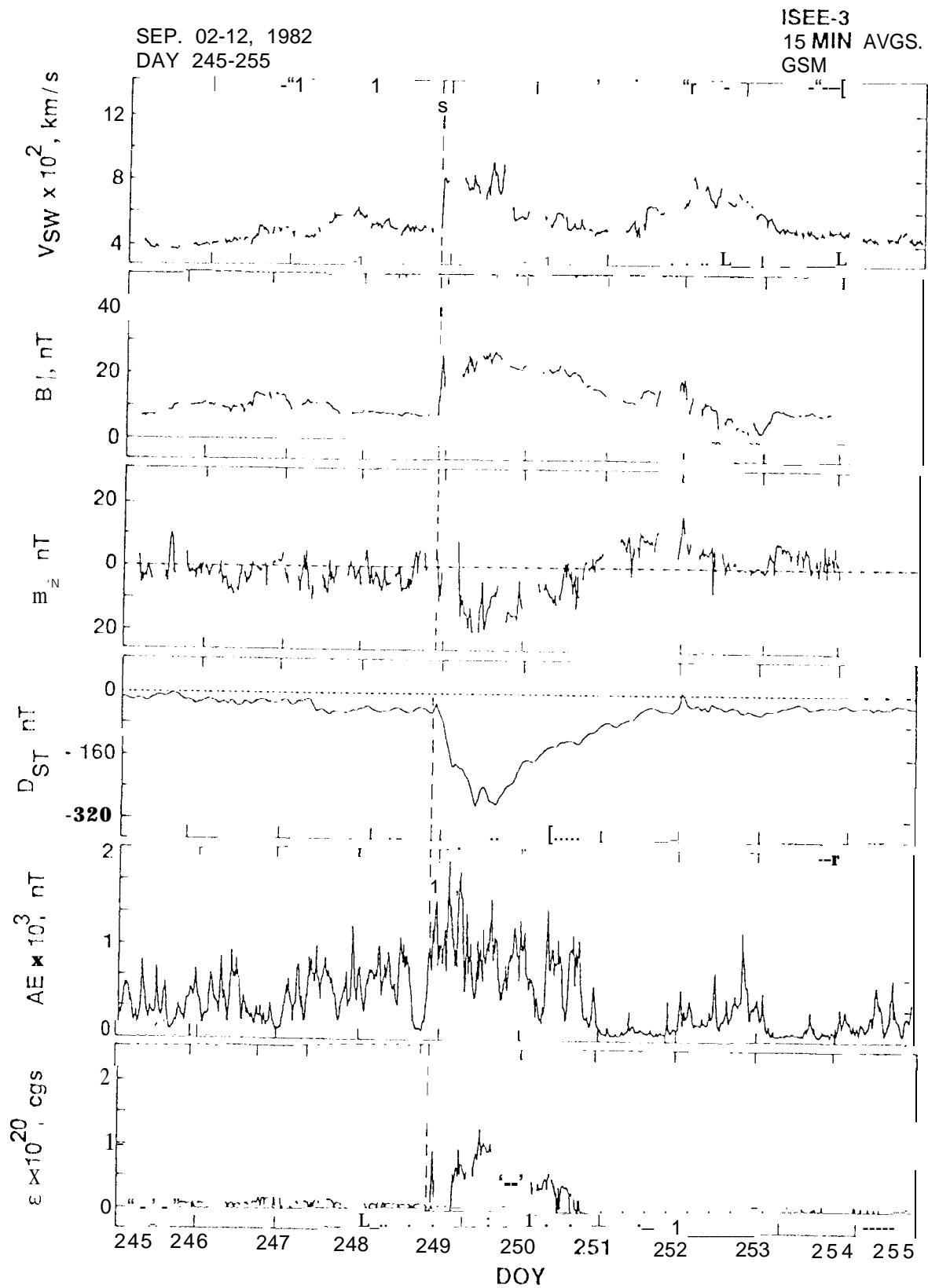
Figure 7

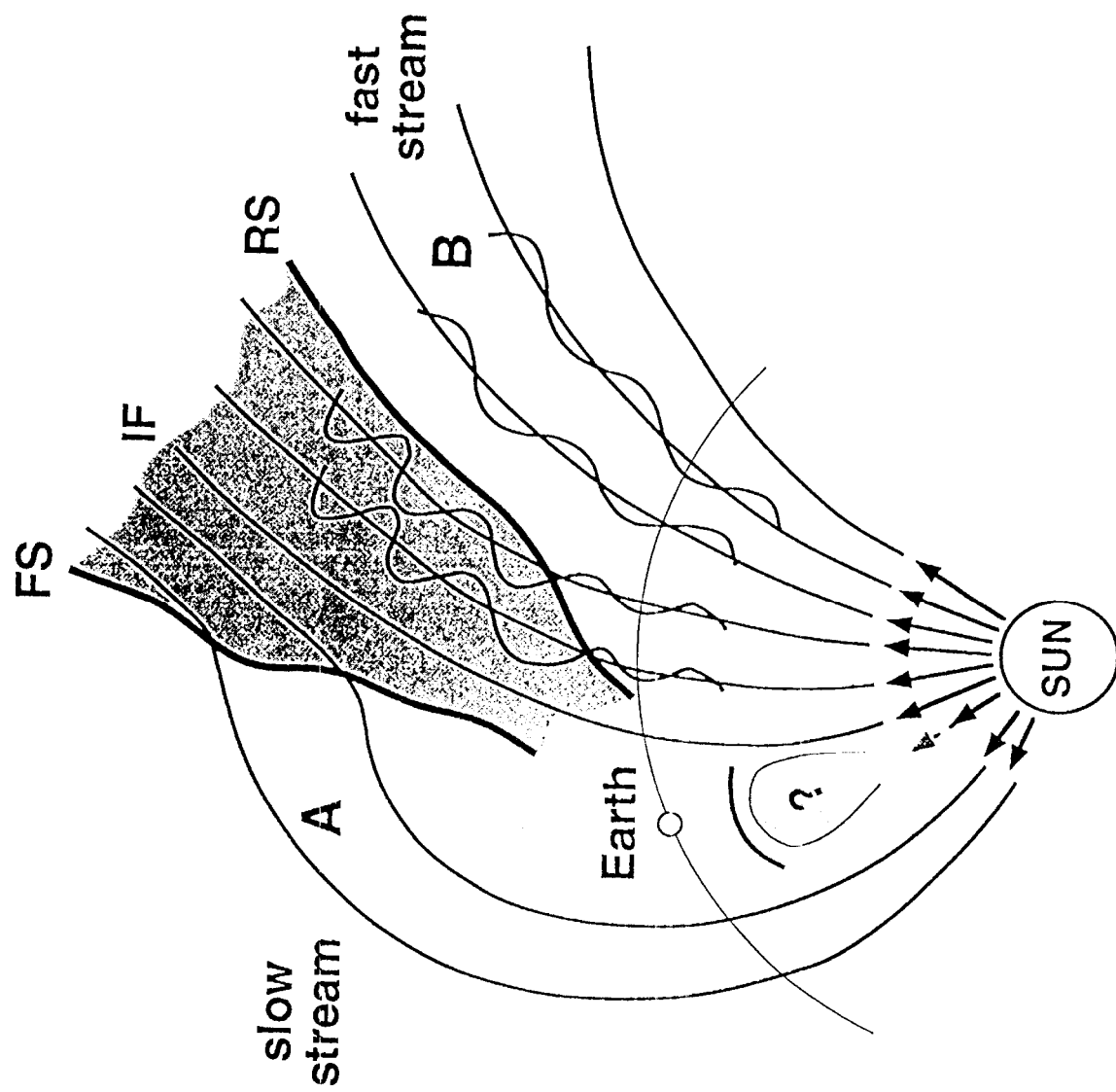# SOLAR - INTERPLANETARY - MAGNETOSPHERE COUPLING
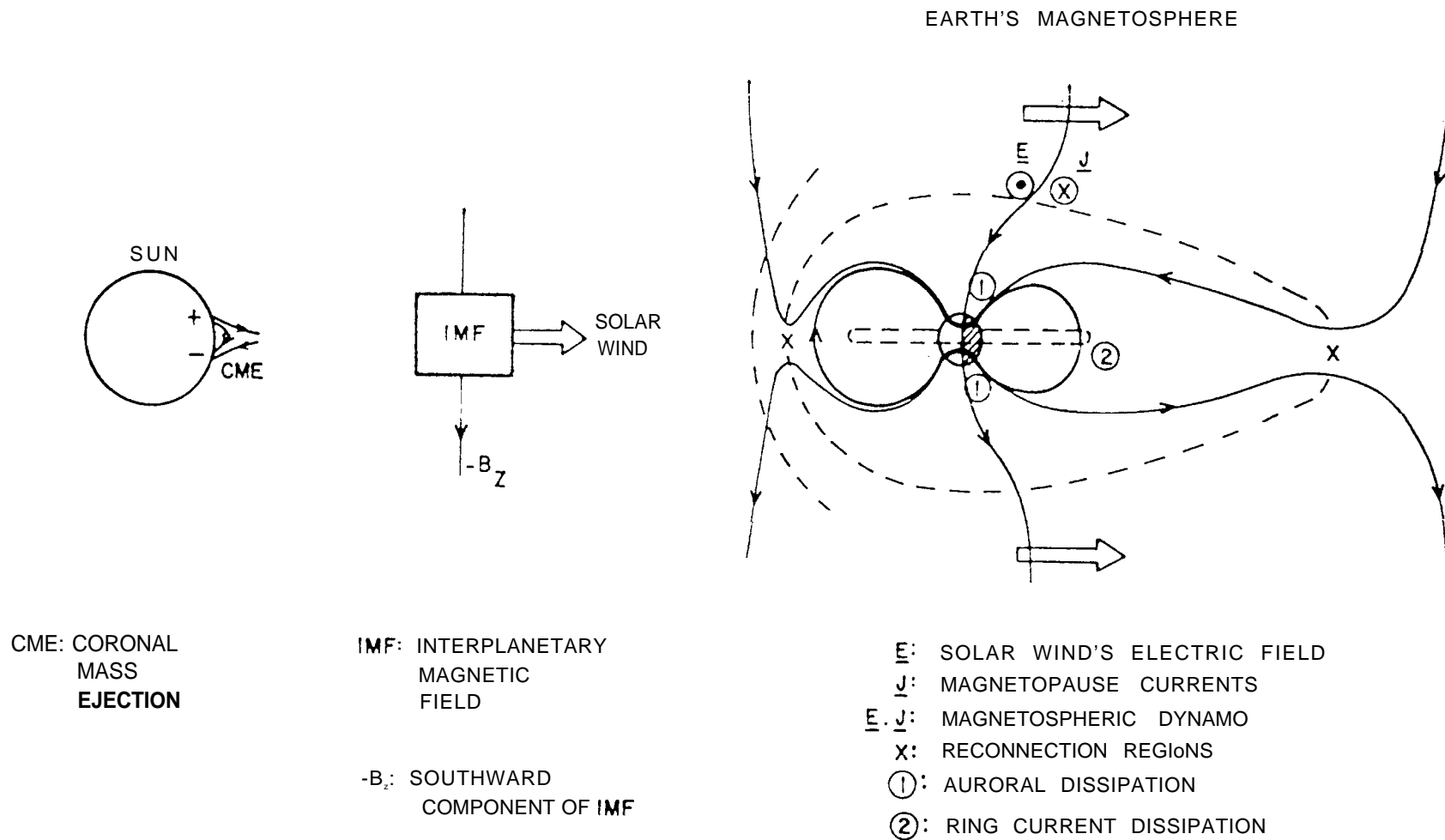
Figure 8

Figure 9

IMP-8
January 24-27, 1974 (Day 024-027)
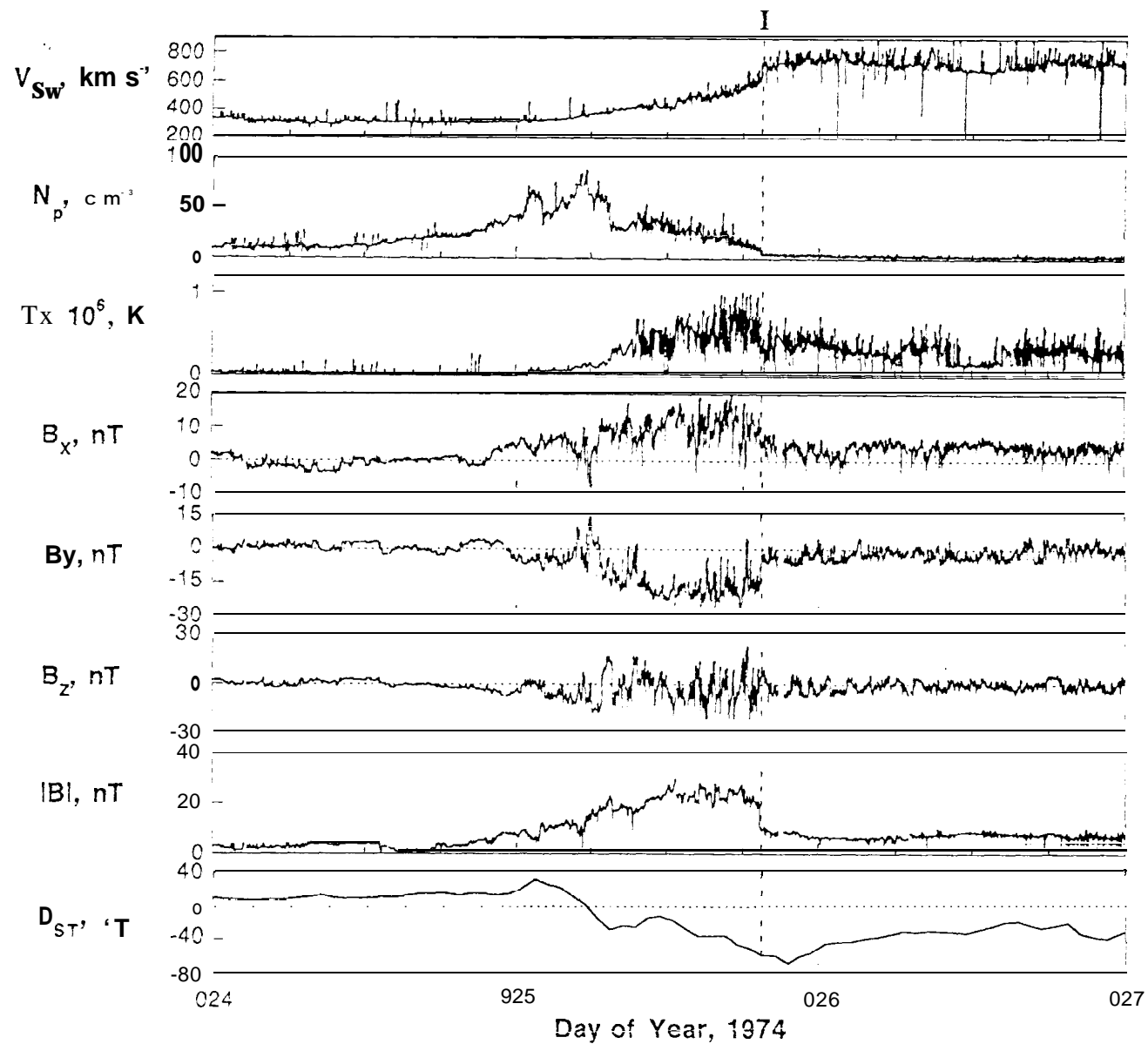
Figure 10

1974 Geomagnetic Indices
(3-hour ap, 1-hour AE and D_{ST})

Day of Year
1974

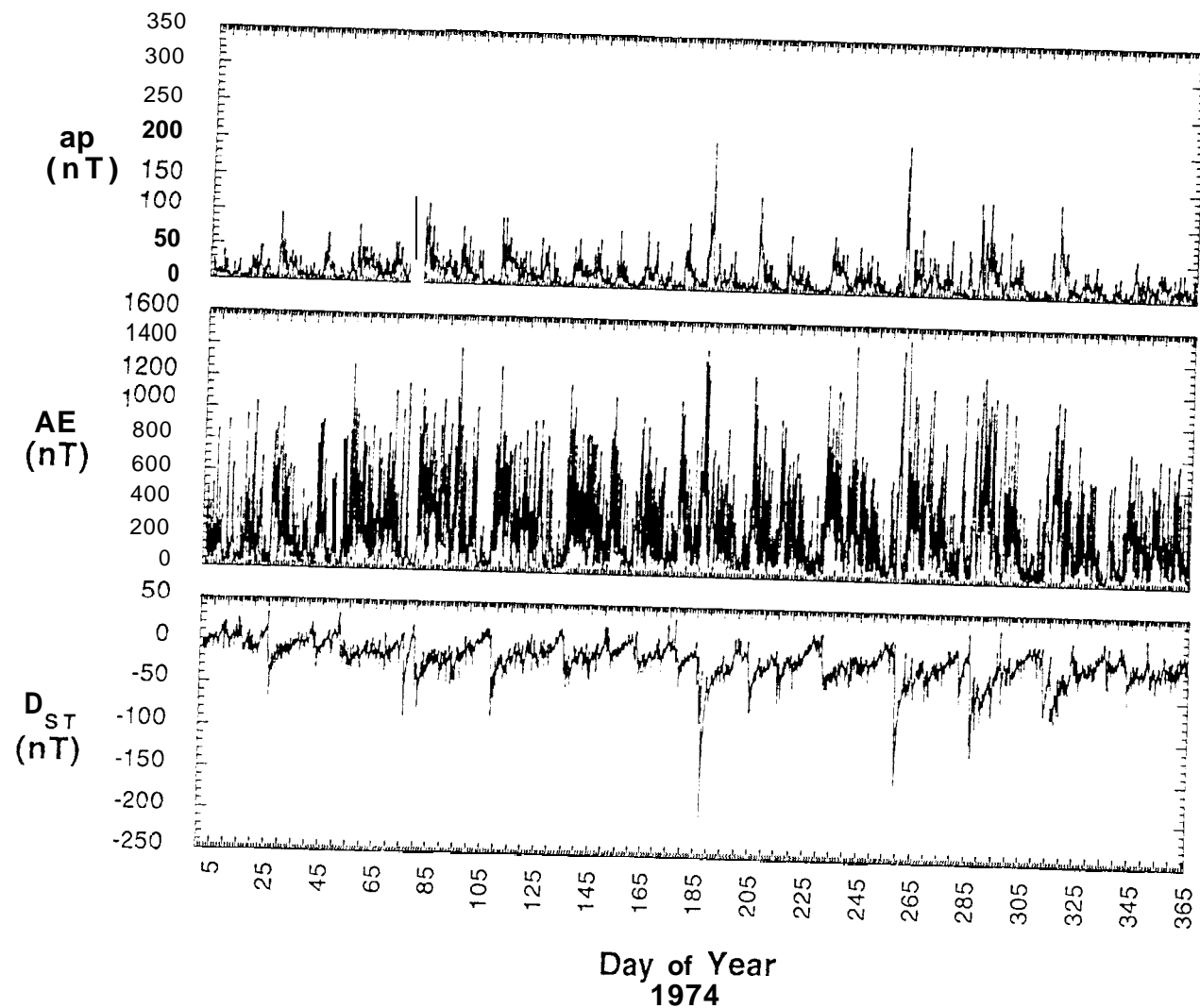**Figure** 11

Recovery Phase of a Magnetic Storm

May 15-18, 1974

Figure 12